Holographic Black Hole Formation and Scrambling in Time-Ordered Correlators

Pratyusha Chowdhury
School of Physics and Astronomy and STAG Research Centre, University of Southampton, SO17 1BJ, Southampton, United Kingdom

Felix M. Haehl and Adrián Sánchez-Garrido
School of Mathematical Sciences and STAG Research Centre, University of Southampton, SO17 1BJ, Southampton, United Kingdom

Ying Zhao
MIT Center for Theoretical Physics—a Leinweber Institute, Massachusetts Institute of Technology, Cambridge, Massachusetts 02139, USA

(Received 24 November 2025; accepted 12 February 2026; published 23 March 2026)

We describe a holographic mechanism for black hole formation via the collision of two shock waves in three-dimensional anti–de Sitter spacetime. In the dual conformal field theory, a two-shock-wave state corresponds to the insertion of two boosted "precursor" operators in complementary Rindler patches. Their operator product expansion is initially described by a universal mean-field spectrum of exchanged states, which is dominated by operator dimensions that grow exponentially in the boost parameter. We propose their mean value as diagnosing the mass of the collision product in the bulk. It crosses the conformal field theory heavy state threshold after two scrambling times, in accordance with expectations about black hole formation in general relativity. Our analysis also allows us to identify the scrambling characteristics usually associated with out-of-time-order correlation functions, using only the internal composition of thermal in-time-order correlators.

DOI: 10.1103/ywfb-82lh

Introduction—While the holographic duality has led to profound insights into quantum gravity, deep puzzles about black hole dynamics remain. To address these microscopically, it is of paramount importance to understand the process of black hole formation in the language of the dual conformal field theory (CFT). It has long been known that black holes in three-dimensional anti–de Sitter (AdS) spacetime [1,2] can be formed in two ways: (i) by gravitational collapse of a dust shell [3–7] and (ii) by collision of shock waves [8–14]. While a holographic understanding in terms of the conformal operator product expansion (OPE) was initiated for the first option in [15], such a perspective has long remained a challenge for the second.

We study this problem in the cleanest holographic setup: the collision of two gravitational shock waves, focused onto each other in an empty global AdS_3 spacetime. We prepare the two-shock "microstate" using CFT primary operators boosted back in time with the Rindler Hamiltonian (so-called precursor operators). For a single operator, Rindler time evolution leads to an exponential spreading of the operator within its conformal family [16,17]. In gravity, this corresponds to an increasingly energetic, nearly null shock wave. However, this kinematical effect by itself cannot lead to black hole formation [18]. In order to set up black hole formation, we require two operators to interact *dynamically* via the OPE; see Fig. 1. In this Letter, we quantify how universal dynamical input leads to an exponential spreading across the space of possible exchanged operators $\mathcal{O}_s$, allowing us to make detailed predictions about the collision product.

The connection between operator growth, information scrambling, and the out-of-time-order correlator (OTOC) is well known [19–21]. In this work, we add a novel and

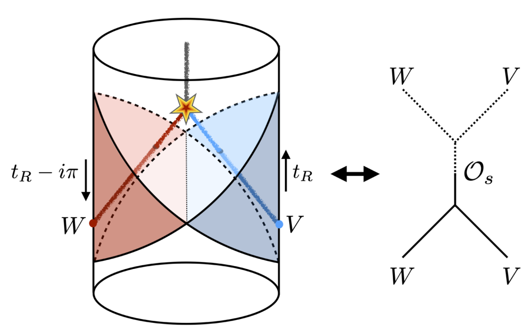

FIG. 1. Kinematic setup: each shockwave originates in one AdS_3 Rindler patch. Information about the collision product is contained in the distribution of exchanged operators in the cross-channel OPE, which depends strongly on the boost.

surprising object to this list of quantum chaos diagnostics: the *in-time-order* four-point correlation function (TOC) of pairwise identical boosted operators. This arises naturally as the self-overlap of the two-shock-wave state. Naively, the TOC's time dependence is trivial; however, its decomposition into irreducible components turns out to give access to time-dependent scrambling behavior normally associated with the OTOC.

Setup—Warmup: One shock wave: Consider a Rindler patch of global AdS_3 with Rindler coordinates (t_R, x). A gravitational shockwave can be prepared in the dual CFT by acting with a primary operator W with conformal weight $1 \ll \Delta_w \ll c$:

$$|\Phi_{W_L}\rangle = W(-t_w - i\pi + i\delta, x_w)|0\rangle, \tag{1}$$

where $t_w < 0$ and $|0\rangle$ is the global vacuum state, which a Rindler observer experiences with an inverse temperature $\beta = 2\pi L_{\mathrm{AdS}}$. In the following, we set the AdS radius $L_{\mathrm{AdS}} = 1$. Note that the argument of the operator is expressed in Rindler coordinates, and, therefore, the shift by $-i\pi$ means that the operator W is inserted in the left Rindler patch (indicated by subscript L), where bulk time is directed in the opposite direction; see Fig. 1. The explicit transformation between plane and Rindler coordinates can be found in Supplemental Material, Sec. A [22]. The small imaginary shift $i\delta$ is required to produce a localized shock wave with finite energy [28].

We increase $-t_w$ starting from 0. This corresponds to evolving the operator into the past with the CFT boost generator $i\partial_{t_R}$. For large $-t_w$, the energy of the excitation localizes along null directions. For example, the expectation value of the light-cone stress-energy tensor is given by a localized shock [28]:

$$\frac{\langle\Phi_{W_L}|T_{++}(t - i\pi, x)|\Phi_{W_L}\rangle}{\langle\Phi_{W_L}|\Phi_{W_L}\rangle} \sim \frac{h_w}{\sin(\delta)}\delta[(t_w + x_w) - (t + x)]. \tag{2}$$

A more microscopic picture is as follows. Under Rindler time evolution, an increasing number of global conformal descendants of W are populated: The primary state "grows" into a coherent superposition of descendants (which are eigenstates of the global Hamiltonian), centered around an increasingly high level (see [16,17,29] for a detailed analysis). In the dual gravitational theory, the small past perturbation evolves into an almost-null shock wave whose proper energy on the $t_R = 0$ slice increases exponentially in $-t_w$. Its gravitational backreaction (on other probes) becomes significant and can be described by a shock-wave geometry after a scrambling time [21,30]:

$$-t_w \sim t_* \sim \log\left(\frac{1}{\Delta_w G_N}\right). \tag{3}$$

Note that this setup never produces a black hole in the bulk, regardless of the value of $-t_w$: The invariant rest mass of the boosted particle remains unchanged. The boosting of the operator is purely kinematical and does not excite boundary graviton degrees of freedom [18]. It is dependent on the choice of a reference frame and can be "undone" by a global isometry transformation. Similarly, in the CFT, the irreducible representation of the Virasoro algebra is invariant and remains the one labeled by W for all times.

Two shock waves: To allow for the possibility of dynamical black hole formation, consider now a two-shock-wave state (Fig. 1):

$$|\Psi_{W_L V_R}\rangle = W(-t_w - i\pi + i\delta, x_w)V(t_v - i\delta, x_v)|0\rangle, \tag{4}$$

where $t_v, t_w < 0$. Rindler time evolution increases the time difference $t \equiv -t_v - t_w > 0$. This corresponds to boosting the operators in the global reference frame: In the bulk, the energy of each particle in the center of mass frame increases exponentially with t. Their collision initially causes a conical defect geometry to form, which can be characterized by its mass M and spin J. This process was studied from a purely gravitational perspective in [9,10]. By analyzing the special geometric features of conical defects in AdS_3, it was found that a Bañados-Teitelboim-Zanelli (BTZ) black hole forms when the mass exceeds the threshold value set by the extremality bound [18,31]:

$$M \geq |J|. \tag{5}$$

This bound is analogous to the so-called Gott condition in flat spacetimes [8]. It was also argued for using holographic quantum circuit models in [32]. See also [33,34] for related recent ideas. As we show below, this condition reads as follows in terms of the parameters of the CFT precursor state:

$$\frac{\sqrt{\Delta_v \Delta_w}}{\sin\delta} e^{(t-|b|)/2} \geq \frac{c}{12} \equiv \frac{1}{8G_N}, \tag{6}$$

where $b = x_v - x_w$ is the impact parameter.

We derive the threshold condition (6) by analyzing the state $|\Psi_{W_L V_R}\rangle$ from a microscopic perspective, using conformal bootstrap tools. Similar precursor states have been analyzed extensively in the study of quantum chaos [21,35,36]. In particular, the scrambling time can be defined as the timescale where naive large-N factorization breaks down because the OTOC $\langle\Psi_{V_L W_R}|\Psi_{W_L V_R}\rangle$ deviates significantly from $\langle VV\rangle\langle WW\rangle$. Crucially, the OTOC computes the overlap of two *differently ordered* states, indicated by L and R labels, referring to the Rindler patch in which operators are inserted, and its path integral representation requires a twice-folded time contour [37]. The difference between the states amplifies over time and leads to a breakdown of large-N factorization after a scrambling time t_*.

In this work, we give a more intrinsic description of the two-shock-wave state $|\Psi_{W_L V_R}\rangle$. We want to ask: *How does the decomposition of the two-shock state into irreducible representations of the Virasoro algebra change over time* [38]? Instead of OTOCs, we consider simply the self-overlap of the (unnormalized) state $|\Psi_{W_L V_R}\rangle$, which we refer to as an *in-time-order four-point function*:

$$\mathcal{F}_{\mathrm{TOC}} \equiv \frac{\langle \Psi_{W_L V_R} | \Psi_{W_L V_R} \rangle}{\langle VV \rangle \langle WW \rangle} \equiv \frac{\mathrm{tr}(W^\dagger W \rho_0^{1/2} V^\dagger V \rho_0^{1/2})}{\mathrm{tr}(V^\dagger V \rho_0)\mathrm{tr}(W^\dagger W \rho_0)}, \qquad (7)$$

where operators in the left Rindler wedge are inserted in an analytically continued fashion halfway around the thermal circle. Indeed, $\rho_0 = (1/Z)e^{-2\pi H}$ is the thermal density matrix seen by a Rindler observer evolving with respect to the Rindler boost generator H. Real-time dependence of operators V and W is implicit in (7), while imaginary time dependence is accounted for by $\rho_0^{1/2}$ factors. This correlator is time ordered, hence the label "TOC." Its value in a large-N chaotic CFT is $\mathcal{F}_{\mathrm{TOC}} \approx 1$ to a good approximation for all times due to large-N factorization. We will not be interested in the value of $\mathcal{F}_{\mathrm{TOC}}$ but in the details of the internal decomposition of the correlator. Perhaps surprisingly, this will unveil scrambling dynamics.

Crossing equation and conformal block decomposition: We begin with a decomposition of the state $|\Psi_{W_L V_R}\rangle$ into irreducible representations of the Virasoro algebra, i.e., Virasoro "OPE blocks" labeled by all possible exchanged primary operators $\mathcal{O}_s$ [41–44]:

$$|\Psi_{W_L V_R}\rangle \propto \sum_{\mathcal{O}_s} C_{wvs} |\mathcal{B}_{WV\mathcal{O}_s}(t_w, x_w; t_v, x_v)\rangle. \qquad (8)$$

The OPE blocks are bilocal operators, furnishing an orthogonal basis of physical exchanges over which we can expand $|\Psi_{W_L V_R}\rangle$ and study its "size" and "spread."

It will be more convenient to analyze the same decomposition by computing the self-overlap, (7). Assuming large-N factorization and a gap in the spectrum of exchanged dimensions, it is clear that $\mathcal{F}_{\mathrm{TOC}} \approx 1$. This is particularly true in CFTs with a gravity dual, where the conformal block associated with the identity operator dominates [45]. We refer to this process ($WW \to \mathbb{1} \to VV$) as *identity dominated t-channel* exchange [46].

By crossing symmetry, we can equivalently decompose $\mathcal{F}_{\mathrm{TOC}}$ into Virasoro conformal blocks in the *s-channel* ($WV \to \mathcal{O}_s \to WV$), directly inherited from (8):

$$1 \approx \mathcal{F}_{\mathrm{TOC}} = \frac{(1-z)^{2h_w}(1-\bar{z})^{2\bar{h}_w}}{z^{h_v+h_w}\bar{z}^{\bar{h}_v+\bar{h}_w}} \sum_{\mathcal{O}_s} C_{wvs}^2 \mathcal{V}_s(z,\bar{z}). \qquad (9)$$

The manipulations leading to this expression can be found in Supplemental Material Sec. B [22]. The s-channel conformal blocks $\mathcal{V}_s(z,\bar{z}) = \langle \mathcal{B}_{WV\mathcal{O}_s} | \mathcal{B}_{WV\mathcal{O}_s} \rangle / \langle VV \rangle \langle WW \rangle$ are functions of conformal cross ratios, which are (for $e^{t-|b|} \gg 1$)

$$z \approx 1 - 4\sin^2(\delta) e^{-t+b}, \qquad \bar{z} \approx 1 - 4\sin^2(\delta) e^{-t-b}; \qquad (10)$$

see Supplemental Material Sec. A for details [22]. The conformal bootstrap program has established powerful tools to analyze the crossing equation (9). In particular, we use the results of Virasoro mean-field theory [48–53], which provides a precise account of the mean-field spectrum $\mathcal{O}_s$ and the couplings C_{wvs}^2; see Supplemental Material Sec. B for a summary [22]. The relevant spectrum of $\mathcal{O}_s$ consists of two parts.

(i) A discrete spectrum of "light" double-twist operators $\mathcal{O}_s^{(m,\bar{m})}$ with integer-spaced conformal weights

$$(h_m, \bar{h}_{\bar{m}}) = (h_v + h_w + m, \bar{h}_v + \bar{h}_w + \bar{m}), \qquad (11)$$

where $m = 1, 2, \ldots, m_*$ and known OPE coefficients (similarly for $\bar{m}$). This spectrum receives anomalous corrections at $\mathcal{O}(1/c)$. The double-twist spectrum ends at the maximum values $(m_*, \bar{m}_*)$, where

$$h_{m_*} = \bar{h}_{\bar{m}_*} = \frac{c-1}{24}. \qquad (12)$$

(ii) A continuous spectrum of "heavy" mean-field operators with conformal weights $(h_s, \bar{h}_s) > (h_{m_*}, \bar{h}_{\bar{m}_*})$. Their average density of states and OPE coefficients are universally determined by the Virasoro fusion kernel. Heavy states are interpreted as dual to black holes with mass and spin [18,54]

$$M = h_s + \bar{h}_s - \frac{c}{12}, \qquad J = \bar{h}_s - h_s. \qquad (13)$$

Equation (9) gives the probability distribution for the decomposition of the state (8) over Virasoro irreducible representations. Like in the one-shock case, boosting the operators probes higher descendant states within a given irrep. A novel feature of the two-shock setup is the fact that the state can now transition into different irreps. The latter effect is captured by the nontrivial dependence of (9) on Rindler time t.

The central observation of this work is as follows: For small Rindler time separation $t \equiv -t_v - t_w$ (low boost), the s-channel decomposition is well described by the exchange of a localized superposition of Virasoro double-twist operators. The expected value of this *double-twist wave packet* grows exponentially in time. Black hole formation in the bulk corresponds to a breakdown of this approximation and the onset of heavy operator exchange.

In the next section, we justify this hypothesis by studying the light exchanges in detail. We show that the light states cease to dominate after a *black hole formation timescale*, i.e., when $t - |b|$ becomes of the order of twice the scrambling time. For previous discussions of this timescale, see [39,55] in the context of scrambling and [40,56] for shock-wave collisions.

Cross-channel analysis: Scrambling in time order—Cross-channel exchange: Global limit: In this subsection, we discuss precisely which operators $\mathcal{O}_s$ dominate in the cross-channel decomposition of $\mathcal{F}_{\rm TOC}$ as a function of the kinematic parameters (t, b, h_v, h_w, δ). We focus on the early-time regime $(1 \ll e^{t-|b|} \ll c^2)$, where only the discrete double-twist light states contribute to the OPE. In this regime, we can safely take the approximation $c \to \infty$ (referred to as "global limit"), effectively extending the cutoff on the double-twist spectrum, $m_*, \bar{m}_* \to \infty$.

The crossing equation (9) can be viewed as the normalization condition for a probability distribution. In the global limit, this distribution is discrete:

$$1 = \left(\sum_{m\geq 0} P_m(h_v, h_w; z)\right)\left(\sum_{\bar{m}\geq 0} P_{\bar{m}}(\bar{h}_v, \bar{h}_w; \bar{z})\right), \qquad (14)$$

where P_m is a probability distribution on the space of s-channel conformal blocks. That is, P_m is the percentage contribution of $\mathcal{O}_s^{(m,\bar{m})}$ defined by (11) (and its descendants) to the correlator $\mathcal{F}_{\rm TOC} \approx 1$. In the global limit, we approximate the Virasoro double-twist conformal blocks by global conformal blocks, which take a simple analytic form (as reviewed in Supplemental Material Sec. B [22]):

$$P_m(h_v, h_w; z) = (1-z)^{2h_w} \frac{z^m}{m!} \frac{(2h_v)_m (2h_w)_m}{(2h_m - m - 1)_m} \times {}_2F_1\left[\begin{matrix} 2h_w + m, 2h_w + m \\ 2h_m \end{matrix} \middle| z\right]. \qquad (15)$$

Here, P_m is the product of universal double-twist OPE coefficients C_{wvs_m} and the global conformal blocks, which are functions of the cross ratio.

The identity (14) and (15) is exact for any choice of kinematic parameters (proven in Supplemental Material Sec. C [22]). However, the relevant range of $(h_m, \bar{h}_{\bar{m}})$ contributing support to the two sums is strongly dependent on the kinematics. Figure 2 shows the probability distribution P_m for fixed (h_v, h_w, δ) as a function of Rindler time difference $t = -t_v - t_w$. The distribution takes the form of a peaked wave packet; the peak moves toward larger values of m exponentially in t, and it broadens at the same time. Let us now quantify this behavior.

The mean value of the exchanged operator dimension is $\mathbb{E}[\Delta_s] = \Delta_v + \Delta_w + \mathbb{E}[m] + \mathbb{E}[\bar{m}]$. This can be computed exactly (see Supplemental Material Sec. C [22]). In the regime of interest $(e^{t-|b|} \gg 1)$, we find

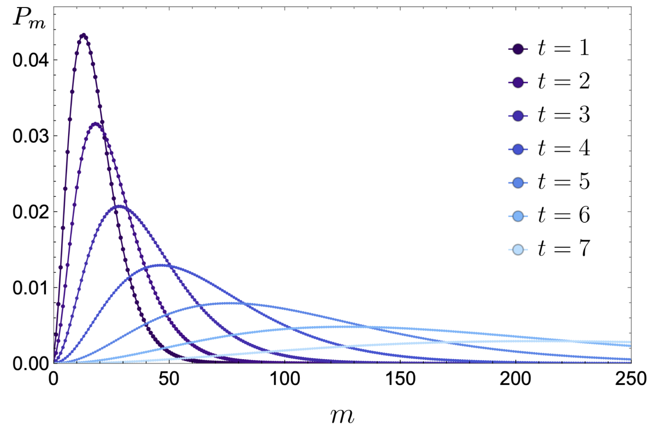

FIG. 2. The (discrete) probability distribution $P_m(h_v, h_w, z)$ on the space of possible s-channel exchange dimensions. The distribution is peaked and moves to higher weights exponentially with time t. We set $h_v = h_w = 1$, $\delta = 0.1$, and $b = 0$.

$$\mathbb{E}[m] \equiv \sum_{m\geq 0} m P_m \approx \frac{1}{\sin(\delta)} \frac{\Gamma(2h_v + \frac{1}{2})\Gamma(2h_w + \frac{1}{2})}{2\Gamma(2h_v)\Gamma(2h_w)} e^{(t-b)/2},$$
$$\mathbb{E}[\bar{m}] \equiv \sum_{\bar{m}\geq 0} \bar{m}\, P_{\bar{m}} \approx \frac{1}{\sin(\delta)} \frac{\Gamma(2\bar{h}_v + \frac{1}{2})\Gamma(2\bar{h}_w + \frac{1}{2})}{2\Gamma(2\bar{h}_v)\Gamma(2\bar{h}_w)} e^{(t+b)/2}. \qquad (16)$$

The symbol $\mathbb{E}[\cdot]$ indicates a (statistical) expectation value with respect to the probability distribution P_m on the space of quasiprimary exchange dimensions. Equivalently, one can formally define a "size" operator $\hat{m}$ which takes the value m on any state in the representation h_m. We could then write the expectation value as $\mathbb{E}[m] = \langle \Psi_{W_L V_R} | \hat{m} | \Psi_{W_L V_R} \rangle / \langle VV \rangle \langle WW \rangle$.

In Fig. 3, we show the numerical evaluation of $\mathbb{E}[m]$: We observe the onset of exponential time dependence with a growth exponent $\frac{1}{2}$, which is independent of the kinematic

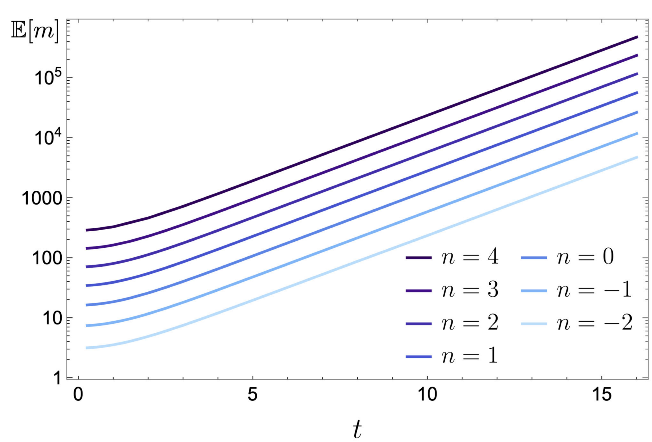

FIG. 3. The mean value of exchanged double-twist dimensions as a function of time. Different lines correspond to different external operator weights $h_v = h_w = 2^n$; $\delta = 0.1$ and $b = 0$.

parameters and consistent with (16). The exponential growth of the mean exchanged operator dimension is a manifestation of the operator growth associated with the two-shock-wave state.

To further corroborate the operator growth picture, we note that the exponential increase of the mean exchanged dimension with time is accompanied by an exponential spreading of the probability distribution's width (see Fig. 2). The two effects occur at an equal rate: The second moments of the distributions are (for $e^{t-|b|} \gg 1$)

$$\sqrt{\mathbb{E}[m^2]} \approx \frac{\sqrt{h_v h_w}}{\sin(\delta)} e^{(t-b)/2}, \qquad \sqrt{\mathbb{E}[\bar{m}^2]} \approx \frac{\sqrt{\bar{h}_v \bar{h}_w}}{\sin(\delta)} e^{(t+b)/2}. \tag{17}$$

These are of the same order as $\mathbb{E}[m]$ and $\mathbb{E}[\bar{m}]$. The tails of the distributions P_m and $P_{\bar{m}}$, therefore, do not grow disproportionately, and we can sensibly identify a mean-localized wave packet even for large t. Higher moments are analyzed in Supplemental Material and behave similarly [22].

Black hole formation: Having seen how the light state s-channel support spreads exponentially in time, we now relax the assumption of infinite central charge and instead take it to be finite but large, $c \gg 1$. This restricts the validity of the global limit taken above.

For values of t small compared to the scrambling time, the approximations of the previous subsection still hold. For simplicity, let us consider scalar operators with $h_v = \bar{h}_v \equiv \frac{1}{2}\Delta_v$ and $h_w = \bar{h}_w \equiv \frac{1}{2}\Delta_w$, and $1 \ll \Delta_{v,w} \ll c$. The Gamma functions in (16) can then be approximated using Stirling's formula. At early times, we propose that the bulk collision produces a conical defect geometry whose expected mass and spin are given by evaluating (13) on the expected values (16) [57]:

$$M + \frac{c}{12} \equiv \mathbb{E}[\Delta_s] \approx \frac{\sqrt{\Delta_v \Delta_w}}{\sin(\delta)} \cosh\left(\frac{b}{2}\right) e^{t/2},$$
$$J \equiv \mathbb{E}[\ell_s] \approx \frac{\sqrt{\Delta_v \Delta_w}}{\sin(\delta)} \sinh\left(\frac{b}{2}\right) e^{t/2}. \tag{18}$$

The threshold for black hole formation corresponds to an extremal geometry with mass $M = |J|$; cf. [18,31]. Using the Brown-Henneaux relation $(c/12) = (1/8G_N)$, this can be written as (6). Once the threshold is reached, the black hole states dominate the s-channel exchange. The associated black hole states have mass $M > |J|$.

Let us understand this from the point of view of the mean-field theory spectrum for $\mathcal{O}_s$. At finite c, the spectrum of discrete "light" double-twist operators $\mathcal{O}_s^{(m,\bar{m})}$ ends sharply at the threshold $(m, \bar{m}) = [m_*(c), \bar{m}_*(c)]$, corresponding to an extremal BTZ black hole; cf. (12). The threshold is reached when the mean of the wave packet of exchanged operators $[\mathbb{E}(m), \mathbb{E}(\bar{m})]$ attains values comparable to $(c/24)$, signaling breakdown of the global limit: The s-channel mean-field support transitions from discrete light states to a continuum of heavy states. These heavy states are precisely those describing the spectrum of BTZ black hole microstates. The onset of the breakdown of light state dominance amounts to the conditions:

$$\text{BTZ threshold:}\ \min\{\mathbb{E}[m_*(c)], \mathbb{E}[\bar{m}_*(c)]\} \approx \frac{c}{24}. \tag{19}$$

In order to overcome the BTZ black hole threshold, it is important for both mean values to reach $(c/24)$; see [18,58]. Comparing with the functional dependence of $\mathbb{E}[m]$ and $\mathbb{E}[\bar{m}]$ in (16), we can translate (19) (or, equivalently, the condition $M = |J|$) into a threshold timescale for black hole formation:

$$t_{\mathrm{BH}} - |b| \sim 2 \times \log\left(\frac{\sin(\delta)}{\sqrt{\Delta_v \Delta_w}} \frac{c}{12}\right). \tag{20}$$

We recognize this as twice the scrambling time and as equivalent to the condition (6) for black hole formation in gravity.

We comment briefly on the approximations made. The threshold derived is not sharp, and some transient behavior takes place around the threshold time. When both $\mathbb{E}[m] \sim \mathcal{O}(c/24) \sim \mathbb{E}[\bar{m}]$, the spectrum $(h_m, \bar{h}_{\bar{m}})$ of light double-twist operators receives large anomalous corrections, and the Virasoro blocks are no longer well approximated by global blocks [53]. This is analogous to the physics of the OTOC around the scrambling time, which is also subject to transient behavior, leading to a breakdown of the large-N approximation and of a simple exponential profile in time [59].

Distribution of descendants: So far, we considered the average primary dimensions $(m, \bar{m})$ of the s-channel wave packet as the parameter determining the exchanged state. This quantity is invariant, as it labels an irreducible orthogonal representation of the Virasoro algebra. Nevertheless, it is also interesting to consider the time-dependent population of global conformal descendants within each such primary family.

In the global limit, for any given primary operator labeled by $(h_m, \bar{h}_{\bar{m}})$, the associated conformal block is built out of an infinite tower of global descendant operators with weights $(h_m + n, \bar{h}_{\bar{m}} + \bar{n})$ for integers $n, \bar{n} \geq 0$ [60]. This decomposition can be viewed as a joint probability distribution $P_{m,n}(h_v, h_w; z)$, which breaks up the primary distribution $P_m(h_v, h_w; z)$ into descendant levels (see Supplemental Material Sec. C2 [22]). Note that this decomposition depends on the choice of a quantization scheme: We need to specify around which point the conformal blocks are expanded, i.e., a reference point for the action of $L_0 + \bar{L}_0$. We choose the canonical expansion into descendants with respect to $z = \bar{z} = 0$ and indicate this with a superscript:

$$P_m(h_v, h_w; z) = \sum_{n\geq 0} P^{(V)}_{m,n}(h_v, h_w; z), \tag{21}$$

and similarly for $P_{\bar{m}}$. The choice of expansion point and map to a canonical configuration in the CFT corresponds to a choice of frame in gravity. The distribution of global descendants depends on these choices.

In the large-c approximation of Virasoro conformal blocks by global blocks, the structure of the global descendants (i.e., the distribution $P^{(V)}_{m,n}$) is well known [61]; it corresponds to the series expansion of the hypergeometric function (15) in powers of the cross ratio. The n th descendant level is characterized by a quantum number $h_{m,n} = h_v + h_w + m + n$ under the global time translation generator L_0 (similarly for $\bar{L}_0$). We can, thus, compute the expectation value of the global energy of the exchanged states analytically. We find (for $c \gg e^{t-|b|} \gg 1$)

$$\mathbb{E}^{(V)}[L_0] = \sum_{m,n}(h_m + n)P^{(V)}_{m,n} \approx h_v + h_w + \frac{h_w}{2\sin^2(\delta)}e^{t-b},$$
$$\mathbb{E}^{(V)}[\bar{L}_0] = \sum_{\bar{m},\bar{n}}(\bar{h}_{\bar{m}} + \bar{n})P^{(V)}_{\bar{m},\bar{n}} \approx \bar{h}_v + \bar{h}_w + \frac{\bar{h}_w}{2\sin^2(\delta)}e^{t+b}. \tag{22}$$

Notably, this growth proceeds at twice the rate of the growth of $\mathbb{E}[m]$ or $\mathbb{E}[\bar{m}]$. We derive this in Supplemental Material Sec. C2 [22] and illustrate it in Fig. 4, which depicts the growth of the exchanged operator in the two-shock-wave state over the space of possible s-channel primaries (labeled by m) and global descendants (labeled by n). A similar notion of global energy increase due to operator growth into descendant levels under Rindler time evolution was previously discussed for a single shock in [17].

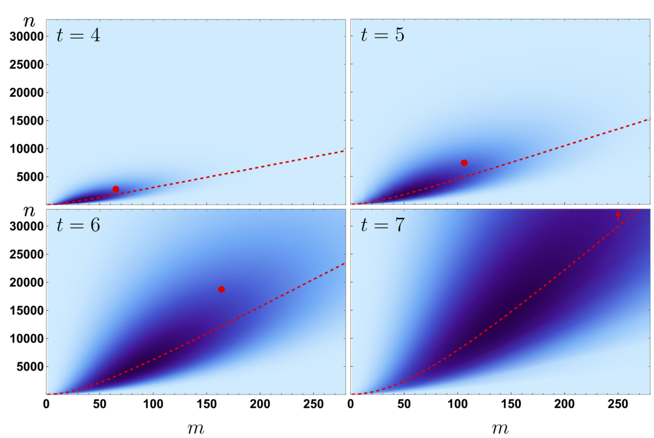

FIG. 4. The joint distribution $P^{(V)}_{m,n}(h_v, h_w, z)$ for $h_v = h_w = 1$ at different times t. Darker colors indicate more support. The dashed lines indicate peak values in the vertical direction for fixed double-twist primary h_m. The dots mark the point $(\mathbb{E}[m], \mathbb{E}^{(V)}[n])$, which determines the global energy $\mathbb{E}^{(V)}[L_0]$.

The global energy of the exchanged state, (22), becomes of the order of $(c/12)$ after one scrambling time t_*. In gravity, this marks the point where gravitational backreaction can no longer be ignored: The spacetime region in the future light cone of the collision point begins to *shrink* due to strong gravity effects [62,63].

Conclusion—In this Letter, we proposed a precise CFT manifestation of black hole formation in AdS_3 via colliding shock waves: We identified a wave packet of mean-field operators exchanged in the cross-channel operator product expansion of two highly boosted precursor operators. The expected value of the distribution of exchanged operators crosses the BTZ black hole threshold at a timescale equal to twice the scrambling time, i.e., when both precursors are sufficiently boosted to generate shock waves. By phrasing this in terms of operator growth within the space of conformal blocks, we discovered scrambling dynamics—normally associated with out-of-time-order correlators—using an in-time-order four-point function diagnostic.

In the future, we plan to report on a detailed analysis of the operator product expansion for timescales exceeding the black hole formation threshold. In this regime, the exchange is dominated by heavy states associated with black holes [33,53]. We expect a qualitatively different distribution of energy among the descendant operators: Excitations of Virasoro (as opposed to global) modes are no longer suppressed by powers of $(1/c)$. These excitations are interpreted as genuine gravitational dressing [18] that cannot be absorbed into global isometry transformations. It is interesting to study the fraction of energy carried by these boundary gravitons and whether this effect translates into a localization of the primary distribution, sharpening the black hole formation transition.

Furthermore, a detailed CFT characterization of the causal structure of the bulk geometry and horizon physics is desirable. The simplicity of geometric horizon formation in gravity suggests that there might be more primitive CFT probes, related to the bulk causal structure, which would detect the same process.

We hope that these insights will pave the way toward a precise definition of operator growth and operator complexity in quantum field theory. Via holography, a detailed microscopic mechanism describing black hole formation may offer key insights into strongly backreacting gravitational dynamics and singularities.

Acknowledgments—The authors are grateful to V. Balasubramanian, A. Belin, C.-M. Chang, C. Chowdhury, S. Collier, B. Czech, T. Hartman, V. Pellizzani, E. Perlmutter, E. Rabinovici, M. Rangamani, A. Rolph, K. Skenderis,

J. Sonner, P. Tadic, and B. Withers for enlightening discussions. F. M. H. and A. S.-G. are supported by United Kingfom Research and Innovation (UKRI) under the United Kingdom government's Horizon Europe Funding Guarantee No. EP/X030334/1. Y. Z. is supported by DOE High Energy DE-SC0012567 and DOE QIS DE-SC0025937. This research was supported in part by Grant No. NSF PHY-2309135 to the Kavli Institute for Theoretical Physics (KITP).

Data availability—No data were created or analyzed in this study.

[1] M. Bañados, C. Teitelboim, and J. Zanelli, Phys. Rev. Lett. **69**, 1849 (1992).
[2] M. Bañados, M. Henneaux, C. Teitelboim, and J. Zanelli, Phys. Rev. D **48**, 1506 (1993).
[3] S. F. Ross and R. B. Mann, Phys. Rev. D **47**, 3319 (1993).
[4] U. H. Danielsson, E. Keski-Vakkuri, and M. Kruczenski, J. High Energy Phys. 02 (2000) 039.
[5] U. H. Danielsson, E. Keski-Vakkuri, and M. Kruczenski, Nucl. Phys. **B563**, 279 (1999).
[6] S. B. Giddings and S. F. Ross, Phys. Rev. D **61**, 024036 (2000).
[7] S. B. Giddings and A. Nudelman, J. High Energy Phys. 02 (2002) 003.
[8] J. R. Gott, Phys. Rev. Lett. **66**, 1126 (1991).
[9] H.-J. Matschull, Classical Quantum Gravity **16**, 1069 (1999).
[10] S. Holst and H.-J. Matschull, Classical Quantum Gravity **16**, 3095 (1999).
[11] J. Polchinski, L. Susskind, and N. Toumbas, Phys. Rev. D **60**, 084006 (1999).
[12] V. Balasubramanian and S. F. Ross, Phys. Rev. D **61**, 044007 (2000).
[13] G. T. Horowitz and N. Itzhaki, J. High Energy Phys. 02 (1999) 010.
[14] E. J. Lindgren, Classical Quantum Gravity **33**, 145009 (2016).
[15] T. Anous, T. Hartman, A. Rovai, and J. Sonner, J. High Energy Phys. 07 (2016) 123.
[16] P. Caputa, J. M. Magan, and D. Patramanis, Phys. Rev. Res. **4**, 013041 (2022).
[17] P. Caputa and S. Datta, J. High Energy Phys. 12 (2021) 188; 09 (2022) 113(E).
[18] C. A. Keller and A. Maloney, J. High Energy Phys. 02 (2015) 080.
[19] Y. Sekino and L. Susskind, J. High Energy Phys. 10 (2008) 065.
[20] J. Maldacena, S. H. Shenker, and D. Stanford, J. High Energy Phys. 08 (2016) 106.
[21] S. H. Shenker and D. Stanford, J. High Energy Phys. 03 (2014) 067.
[22] See Supplemental Material at http://link.aps.org/supplemental/10.1103/ywfb-82lh for further technical details, which includes Refs. [23–27].
[23] Y. Kusuki, arXiv:2412.18307.
[24] A. B. Zamolodchikov, Sov. Phys. JETP **63**, 1061 (1986), https://ui.adsabs.harvard.edu/abs/1986JETP...63.1061Z/.
[25] S. Collier, A. Maloney, H. Maxfield, and I. Tsiares, J. High Energy Phys. 07 (2020) 074.
[26] A. Belin and J. de Boer, Classical Quantum Gravity **38**, 164001 (2021).
[27] A. L. Fitzpatrick and J. Kaplan, J. High Energy Phys. 10 (2012) 032.
[28] N. Afkhami-Jeddi, T. Hartman, S. Kundu, and A. Tajdini, J. High Energy Phys. 03 (2019) 201.
[29] P. Caputa and D. Ge, J. High Energy Phys. 06 (2023) 159.
[30] M. Banados, AIP Conf. Proc. **484**, 147 (1999).
[31] M. Banados, C. Teitelboim, and J. Zanelli, Phys. Rev. Lett. **69**, 1849 (1992).
[32] F. M. Haehl and Y. Zhao, J. High Energy Phys. 07 (2023) 184.
[33] D. Das, S. Datta, and S. Pal, Phys. Rev. D **98**, 101901 (2018).
[34] S. Banerjee and G. Vos, J. High Energy Phys. 10 (2025) 011.
[35] D. A. Roberts, D. Stanford, and L. Susskind, J. High Energy Phys. 03 (2015) 051.
[36] S. H. Shenker and D. Stanford, J. High Energy Phys. 05 (2015) 132.
[37] I. L. Aleiner, L. Faoro, and L. B. Ioffe, Ann. Phys. (Amsterdam) **375**, 378 (2016).
[38] A related approach is to quantify the operator size of the two-shock state by computing a probe correlator $\langle\Psi_{W_L V_R}|\mathcal{O}(t_1)\mathcal{O}(t_2)|\Psi_{W_L V_R}\rangle$. This is again an OTOC, now requiring a thrice-folded time contour [39,40].
[39] F. M. Haehl and M. Rozali, Phys. Rev. Lett. **120**, 121601 (2018).
[40] F. M. Haehl, A. Streicher, and Y. Zhao, J. High Energy Phys. 08 (2021) 134.
[41] B. Czech, L. Lamprou, S. McCandlish, B. Mosk, and J. Sully, J. High Energy Phys. 07 (2016) 129.
[42] J. de Boer, F. M. Haehl, M. P. Heller, and R. C. Myers, J. High Energy Phys. 08 (2016) 162.
[43] A. L. Fitzpatrick, J. Kaplan, D. Li, and J. Wang, J. High Energy Phys. 07 (2017) 092.
[44] F. M. Haehl and K.-W. Huang, J. High Energy Phys. 02 (2026) 030.
[45] T. Hartman, arXiv:1303.6955.
[46] In the case of the OTOC, identity dominance is rather subtle to establish due to nonconvergence of the OPE [47]. In our setup, using $\mathcal{F}_{\mathrm{TOC}}$, the OPE converges even as $z \to 1^-$. Identity dominance is, thus, justified as long as the spectrum of t-channel exchanges is sufficiently gapped.
[47] C.-M. Chang, D. M. Ramirez, and M. Rangamani, J. High Energy Phys. 03 (2019) 068.
[48] B. Ponsot and J. Teschner, arXiv:hep-th/9911110.
[49] B. Ponsot and J. Teschner, Commun. Math. Phys. **224**, 613 (2001).
[50] S. Jackson, L. McGough, and H. Verlinde, Nucl. Phys. **B901**, 382 (2015).
[51] C.-M. Chang and Y.-H. Lin, J. High Energy Phys. 10 (2016) 068.
[52] S. Caron-Huot, J. High Energy Phys. 09 (2017) 078.
[53] S. Collier, Y. Gobeil, H. Maxfield, and E. Perlmutter, J. High Energy Phys. 05 (2019) 212.
[54] J. D. Brown and M. Henneaux, Commun. Math. Phys. **104**, 207 (1986).
[55] T. Anous and F. M. Haehl, J. High Energy Phys. 08 (2020) 002.
[56] F. M. Haehl and Y. Zhao, Phys. Rev. D **104**, L021901 (2021).

[57] We choose the ground state energy of global AdS_3 as $-(c/12)$. Below-threshold geometries, thus, have negative mass.

[58] Our analysis here assumes that neither $\Delta_{v,w}$ nor b scale with c.

[59] D. A. Roberts and D. Stanford, Phys. Rev. Lett. **115**, 131603 (2015).

[60] Note that irreps of the global conformal group are labeled by the eigenvalue of the Casimir operator: $\mathcal{C} = L_0^2 - \frac{1}{2}(L_1 L_{-1} + L_{-1} L_1) = h_m(h_m - 1)$.

[61] F. A. Dolan and H. Osborn, Nucl. Phys. **B599**, 459 (2001).

[62] F. M. Haehl and Y. Zhao, J. High Energy Phys. 09 (2022) 002.

[63] This effect can also be understood using quantum circuit models [62], which implement the interplay between the spreading of each precursor operator's effect inside a causal light cone and the ballistic spread of its scrambling dynamics inside a "butterfly cone" [35,64].

[64] M. Mezei and G. Sárosi, J. High Energy Phys. 01 (2020) 186.